COMMUNICATION

A spin crossover ferrous complex with ordered magnetic ferric anions

Olivier Roubeau,*[a] Eva Natividad,[b] Marco Evangelisti[a]

Received (in XXX, XXX) Xth XXXXXXXXX 20XX, Accepted Xth XXXXXXXXX 20XX
DOI: 10.1039/c0xx00000x

The first tetrahaloferrate spin crossover compound, $[Fe(Metz)_6](FeBr_4)_2$, is reported. The $FeBr_4^-$ ions form ferromagnetically coupled 1D stacks and exhibit an antiferromagnetic order at 2.2 K, that coexists with the gradual spin crossover centred at 165 K.

Designing magnetic materials with two or more potential functions resulting from different physical properties, either in synergy or totally un-correlated, has become a strong topic in chemical and materials sciences.[1] Spin crossover (SCO) compounds have been the source of a number of multifunctional synthetic systems,[2] as the SCO phenomenon itself, in particular with Fe(II) coordination systems for which the low-spin (LS) state is purely diamagnetic, gives access to concomitant drastic variations in magnetic, optical and dielectric responses,[3] and can be implemented into liquid crystalline or gel phases.[4] An elegant synthetic strategy towards multifunctional materials is to build two-network hybrid crystalline solids, and this has been particularly efficient with one of the networks having a 2D layered structure thus allowing intercalation of molecular, 1D or 2D species.[5] SCO complexes were only recently successfully integrated into 2D and 3D ferromagnetic magnetic oxalate anionic networks,[6] using mononuclear Fe(III) complexes bearing chelating ligands. Fe(II) systems have so far eluded such success, likely because of a combination of inadequate charge, easier oxidation and greater sensitivity to environmental changes of the conditions favouring SCO. On the other hand, Fe(II) SCO complexes were successfully integrated into materials with lower dimensionality, as cations[7] or spin component[8] of Single-Chain-Magnets, although in the latter case SCO was not maintained. With the goal of obtaining simpler truly molecular SCO compound with interesting magnetic properties at low temperatures, we have used paramagnetic tetrabromoferrate(III) anions in conjunction with 1-methyltetrazole (Metz). Indeed, the $[Fe^{II}(N_{tz})_6]$ coordination core (tz = substituted tetrazole) probably represents the most-widely studied type of SCO compounds, while providing the highest probability of occurrence of SCO.[9] On the other hand, tetrahaloferrate(III) ions have been widely used in molecular conductors[10] and can interact ferromagnetically depending on their stacking,[11] potentially resulting in ferromagnetic order.[12] We report here the first SCO compound with a tetrahaloferrate(III) anion, $[Fe(Metz)_6](FeBr_4)_2$ (**1**) and its analogue $[Zn(Metz)_6](FeBr_4)_2$ (**2**), in which the $FeBr_4^-$ ions form ferromagnetically coupled 1D stacks and order antiferromagnetically at 2.2 K.

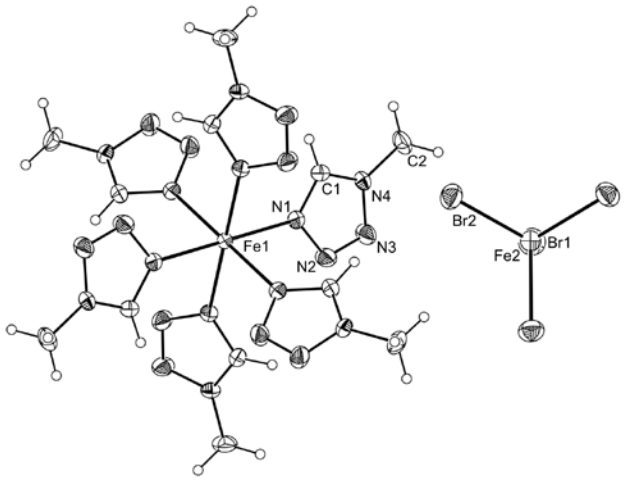

Fig. 1 ORTEP view at 30 % probability of the structure of **1** at 296 K along the *c* axis. Only non-hydrogen atoms of the asymmetric unit are labelled.

Red crystals of **1** are readily obtained in high yield from the reaction of Metz, ferrous and ferric bromides in a 6:1:2 molar ratio in ethanol. The Zn(II) analogue, $[Zn(Metz)_6](FeBr_4)_2$ (**2**) is easily obtained replacing ferrous bromide by zinc bromide. This simple synthetic route uses $FeBr_4^-$ ions formed in-situ from $FeBr_3$ in the presence of bromide anions, thus avoiding the addition of a pre-formed salt that would add an unwanted cation to the system. In addition, the presence of Fe(III) ions in solution likely prevents Fe(II) ions from aerobic oxidation, as no addition of ascorbic acid is required for the synthesis of **1**.

Single-crystal X-ray analysis at room temperature reveals **1** crystallizes in the trigonal *P*–3 space group with one $[Fe(Metz)_6]^{2+}$ cation and two $FeBr_4^-$ ions per cell. The asymmetric unit contains two Fe sites on special positions with 6 and 3-fold multiplicity respectively, one Metz molecule and two Br atoms. The $[Fe(Metz)_6]^{2+}$ cation consists of Fe1 atom surrounded by six Metz ligands, identical by symmetry, coordinated through N1 with a Fe–N1 bond distance of 2.186(2) Å, indicative of a HS state.[13] The resulting FeN_6 octahedron is only slightly distorted with N–Fe–N angles of 88.88(9) and 91.12(9)º. Each methyl group points towards another from a neighbouring complex, with a C2···C2' separation of 3.354 Å. The $FeBr_4^-$ ion has an almost perfect tetrahedral geometry around the Fe2 atom with similar Fe2–Br1 and Fe2–Br2 bond distances, at respectively 2.3240(11) and 2.3437(5) Å, and Br1–Fe–Br2 and Br2–Fe–Br2 bond angles, at respectively 109.70(2) and

109.24(2)°, in accord with simple salts of this anion.[14] Each $FeBr_4^-$ ion forms hydrogen bonds with a tetrazole aromatic hydrogen of three neighbouring $[Fe(Metz)_6]^{2+}$ complexes, with a Br2···H1 distance of 3.811(4) Å (Fig. S2). The two $FeBr_4^-$ in the cell have their Fe2–Br1 bond parallel to the *c* axis, in opposite directions, with a Fe···Fe separation of 7.489 Å and a Br2···Br2 short contact of 4.472 Å (Fig. S3). The $FeBr_4^-$ ions are stacked along the *c* axis in a perfectly eclipsed conformation (Fig. S3), with a Fe···Fe separation of 6.9577(1) Å. There are rather short Br1···Br2 and Br1···Fe2 contacts between these stacked $FeBr_4^-$ at respectively 4.431 and 4.634 Å (Figs. S3 and S4). A similar structure is obtained at 104 K, with no change in space group but with a reduction of both *a* and *c* axes, resulting in a cell volume decrease of 6.2%. This reduction likely involves both the normal thermal contraction and the effect of the SCO occurring at the Fe1 site. Indeed, the Fe1–N1 bond distance has decreased by 8.4% at 2.003(2) Å, now typical of a LS state.[13] The Fe···Fe separation along the $FeBr_4^-$ stacks is reduced, to 6.7980(14) Å, with shorter Br1···Br2 and Br1···Fe2 contacts, at respectively 4.287 and 4.474 Å. The inter-stack Fe···Fe separation is also reduced, to 7.337 Å. The Zn(II) analogue **2** is isostructural to **1** at room temperature, with very similar stacking of the $FeBr_4^-$ ions (see Table S1 and Fig. S5).

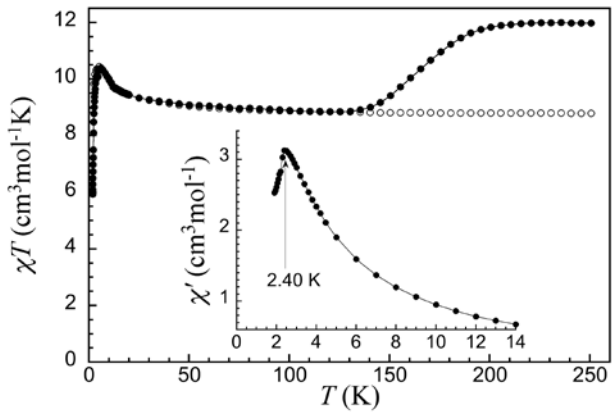

Fig. 2 χT vs. *T* plot for compounds **1** (full circles) and **2** (empty circles) showing the process of SCO in **1** and a similar ferromagnetic signature down to 6 K for both **1** and **2**. Inset: low-temperature in-phase as susceptibility of **1** at 15 Hz.

Magnetic properties of both compounds were determined in the range 1.9-250 K and are sketched in Figure 2 as a χT vs. *T* plot, χ being the molar magnetic susceptibility. The value of χT at 250 K for compound **1**, at 12.0 $cm^3mol^{-1}K$, agrees with that expected for one Fe(II) ion in the $S = 2$ HS state and two Fe(III) $S = 5/2$ spins (11.75 $cm^3mol^{-1}K$). A decrease of χT is observed upon cooling from about 210 K reaching a minimum at around 120 K at 8.84 $cm^3mol^{-1}K$, value in accord with only two Fe(III) $S = 5/2$ spins (8.75 $cm^3mol^{-1}K$). Clearly this decrease corresponds to the almost complete thermal SCO exhibited by the Fe1 site, and centred at ca. 170 K. Indeed, compound **2**, in which this site is occupied by a diamagnetic Zn(II) ion, exhibits similar χT values, at 8.79-8.86 $cm^3mol^{-1}K$, from 250 down to about 115 K. The gradual SCO behaviour of **1** is similar in shape to that of the BF_4^- or ClO_4^- derivatives, but it occurs ca. 100 K higher in temperature.[9] Moreover, the presence of a single Fe(II) crystallographic site in **1** results in a complete SCO, as opposed to the 50% SCO associated with the presence of two Fe sites of these other derivatives with tetrahedral anions.[9,14] Below 120 K, both compounds **1** and **2** exhibit a similar increase of χT, indicative of the presence of ferromagnetic interactions, to reach a maximum value of 10.38 $cm^3mol^{-1}K$ at 6 K. Below 6 K, a sharp decrease is then observed, to reach 6.09 $cm^3mol^{-1}K$ at 1.9 K for **1**. The increase of χT can reasonably be ascribed to a ferromagnetic coupling of the paramagnetic $FeBr_4^-$ ions in the stacked chains along the *c* axis.[11] The drop below 6 K, associated with a marked maximum at 2.40 K in χ' (inset in Fig. 2) likely corresponds to an antiferromagnetic order of the $FeBr_4^-$ ions.

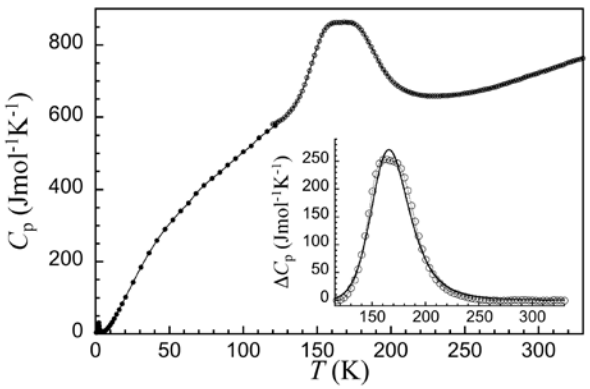

Fig. 3 The molar heat capacities of **1** showing a broad hump associated with the SCO. Full/empty symbols: relaxation/DSC data. Inset: Excess heat capacities associated with the SCO in **1**. The full line is a fit to the domain model of Sorai (see text and SI).

The molar heat capacity (C_p) of **1** was determined from differential scanning and semi-adiabatic relaxation calorimetry for the temperature ranges 120-330 K and 0.3-130 K, respectively. We associate the broad hump covering 130-220 K (Fig. 3) to the thermal signature of a gradual SCO, in good agreement with the magnetic data. The excess enthalpy and entropy associated with the SCO in **1** were deduced by integration of the excess heat capacity (inset in Fig. 3) and arise to 13.1 $kJmol^{-1}$ and 77.8 $Jmol^{-1}K$, respectively. These figures are rather large, in particular the excess entropy well above the electronic component $R\ln5$, which is often taken as an indication of the cooperativeness of the SCO phenomenon. Nevertheless, reproducing the experimental data with the so-called domain model[15] gives a domain size *n* of 1.47, in agreement with a poorly-cooperative system[15,16] and thus with the shape of magnetic and thermal signature of the SCO in **1**.

The low-temperature heat capacity is characterized by an applied-field dependent contribution, whose most prominent feature is a lambda-like peak centred at $T_N \cong 2.2$ K for zero-field (Fig. 4). This feature indicates a phase transition to long-range magnetic order, nicely corroborating the magnetic data. The fact that the peak is not affected by fields lower than $B_0 = 0.5$ T points to antiferromagnetic ordering. Larger fields gradually decouple the magnetic interactions and for, *e.g.* $B_0 = 7$ T in Fig. 4, the experimental C_p is satisfactorily modelled with the Schottky heat capacity (solid line), which results from summing the contributions of two non-interacting Fe(III) ion spins. At high temperatures, the experimental C_p is dominated by non-magnetic contributions arising from thermal vibrations of the lattice, which

can be modelled with the Debye function (dashed line) yielding a value of θ_D = 43.4 K for the Debye temperature, which is in the range of values observed for this class of molecular compounds.[17] By subtracting the lattice contribution from the zero-field C_p, we are left with the tail of the magnetic ordering heat capacity (C_m) that has a characteristic T^{-2} dependence at high temperatures (empty markers for T > 3 K). On the other side of the peak, we note an upward curvature below 0.5 K, which can be understood as an excess C_p added on top of the zero-field peak data. As indicated in Fig. 4 (empty markers for T < 0.5 K), we have used a linear-T extrapolation, as would be appropriate for the spin-wave contribution for an isotropic 1D antiferromagnet.[18] The resulting low values for the excess C_p, combined with its slight dependence on the applied field, suggests that this feature originates from the splitting of residual HS Fe(II) ions by the internal ordering field. Finally, associating the spin-wave extrapolation to C_m, we obtain the zero-field magnetic entropy, using $S_m(T) = \int C_m(T)/T dT$. The inset of Fig. 4 shows that $S_m(T)$ beautifully tends at high T to the full content corresponding to two Fe(III) S = 5/2 spins, *i.e.* $2xR\ln(2S+1) = 3.58R$, corroborating our initial hypothesis that the ordering involves Fe(III) spins solely.

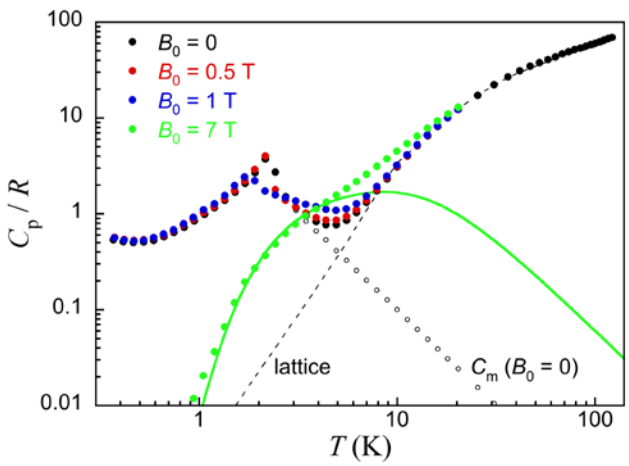

Fig. 4 The molar heat capacity of **1**, normalized to the gas constant R and collected for the indicated applied fields. Plotted also are: Schottky contribution for B_0 = 7 T (solid line), spin-wave linear-T extrapolation and zero-field $C_m \propto T^{-2}$ (both as empty markers), obtained by subtracting the lattice contribution (dashed line) from the total zero-field heat capacity. Inset: Zero-field magnetic entropy of **1**.

The aforementioned experiments evidence that ferro- and antiferromagnetic interactions are both contributing in the Fe(III) magnetic ordering process. We can push further our analysis by making use of the recent theoretical work by Ito *et al.*[11] that sheds light by predicting ferromagnetism for the direct *d-d* exchange interaction along the same 1D chain topology as in **1**. According to their model, we envisage J/k_B = 0.22 K for such an intrachain coupling. Next, from the value of 2.2 K as the temperature for the ordering process between the chains, we can estimate the interchain coupling J' by using the Oguchi's model,[19] obtaining $|J'|/|J| \approx 0.6$, and therefore $J'/k_B \approx -0.13$ K on basis of the above.

In summary, we have shown that using simple tetrabromoferrate(III) ions formed in-situ allows the isolation of the first spin crossover (SCO) compound with paramagnetic tetrahaloferrate ions. In this original material, the spin crossover phenomenon of the cationic sublattice coexists with a magnetic order of the anionic sub-lattice. The strategy can certainly be expanded to many spin crossover systems based on a cationic complex, and could thus open a synthetic path to a whole new range of multifunctional spin crossover-based materials.

Notes and references

[a] *Instituto de Ciencia de Materiales de Aragón (ICMA), CSIC - Universidad de Zaragoza, Departamento de Fisíca de la Materia Condensada, Pl. San Francisco s/n, 50009 Zaragoza, Spain; Fax: 34 976 76123; Tel: 34 976 762461; E-mail: roubeau@unizar.es*

[b] *Instituto de Ciencia de Materiales de Aragón (ICMA), CSIC - Universidad de Zaragoza, Sede Campus Río Ebro, María de Luna, 3, 50018 Zaragoza, Spain.*

† Electronic Supplementary Information (ESI) available: synthetic details, SEM images of **1**, relevant distances/angles for **1** and **2**, additional views of the structures of **1**-**2**, cifs of **1**-**2**. See DOI: 10.1039/b000000x/

‡ Crystal data for **1**: $[C_{12}H_{24}FeN_{24}](FeBr_4)_2$. Data were collected at 296 / 104 K, trigonal, space group P–3 (no. 147) with a = 12.683(2) / 12.9487(1) Å, c = 6.7890(14) / 6.9577(1) Å, V = 947.0(3) / 1010.30(2) Å^3, Z = 1, ρ_{calcd} = 2.299 / 2.155 g/cm^3, μ = 10.523 / 9.017 mm^{-1}. 26453 / 16943 reflections were measured, 1342 / 1383 of which were independent. Refinement converged at final w$R2$ = 0.0978 / 0.0578, $R1$ = 0.0359 / 0.0280 and S = 1.080 / 0.861 (for 1339 / 903 reflections with $I > 2\sigma(I)$). Crystal data for **2**: $[C_{12}H_{24}ZnN_{24}](FeBr_4)_2 \cdot 2$. Data were collected at 296 K, trigonal, space group P–3 (no. 147) with a = 12.9404(4) Å, c = 6.9522(3) Å, V = 1008.20(6) Å^3, Z = 1, ρ_{calcd} = 2.176 g/cm^3, μ = 9.270 mm^{-1}. 6659 reflections were measured, 1382 of which were independent. Refinement converged at final w$R2$ = 0.0974, $R1$ = 0.0477 and S = 1.057 (for 1060 reflections with $I > 2\sigma(I)$).

[1] E. Coronado, J. R. Galán-Mascarós, C. J. Gómez-García and V. Laukhin, *Nature*, 2000, **408**, 447-449; J. S. Miller, *Angew. Chem. Int. Ed.*, 2003, **42**, 27-29.

[2] A. B. Gaspar, V. Ksenofontov, M. Seredyuk and P. Gütlich, *Coord. Chem. Rev.*, 2005, **249**, 2661-2676 ; A. Bousseksou, G. Molnár, L. Salmon and W. Nicolazzi, *Chem. Soc. Rev.*, 2011, **40**, 3313-3335.

[3] P. Gütlich, A. Hauser, H. Spiering, *Angew. Chem. Int. Ed.*, 1994, **33**, 2024-2054.

[4] A. B. Gaspar, M. Seredyuk and P. Gütlich, *Coord. Chem. Rev.*, 2009, **253**, 2399-2413 ; O. Roubeau, A. Colin, V. Schmitt and R. Clérac, *Angew. Chem. Int. Ed.*, 2004, **43**, 3283-3286.

[5] E. Coronado, C. Martí-Gastaldo, E. Navarro-Moratalla, A. Ribera, S. J. Blundell and P. J. Baker, *Nature Chem.*, 2010, **2**, 1031-1036; M. Clemente-León, E. Coronado, C. Martí-Gastaldo and F. M. Romero, *Chem. Soc. Rev.*, 2011, **40**, 473-497; G. Rogez, C. Massobrio, P. Rabu and M. Drillon, *Chem. Soc. Rev.*, 2011, **40**, 1031-1058.

[6] M. Clemente-León, E. Coronado, M. López-Jordà, C. Desplanches, S. Asthana, H. Wang and J-F. Létard, *Chem. Sci.*, 2011, **2**, 1121-1127; M. Clemente-León, E. Coronado, M. López-Jordà and J. C. Waerenborgh, *Inorg. Chem.*, 2011, **50**, 9122-9130.

[7] J. H. Yoon, D. W. Ryu, S. Y. Chi, H. C. Kim, E. K. Koh, J. Tao and C. S. Hong, *Chem. Commun.*, 2011, **47**, 10416-10418.

[8] T. S. Venkatakrishnan, S. Sahoo, N. Bréfuel, C. Duhayon, C. Paulsen, A-L. Barra, S. Ramasesha, J-P. Sutter, *J. Am. Chem. Soc.*, 2010, **132**, 6047-6056.

[9] G. Aromí, L. A. Barrios, O. Roubeau and P. Gamez, *Coord. Chem. Rev.*, 2011, **255**, 485-546.

[10] E. Coronado and P. Day, *Chem. Rev.*, 2004, **104**, 5419-5448.

[11] M. Takenaka, T. Kawakami, A. Ito, K. Kinoshita, Y. Kitagawa, S. Yamanaka, K. Yamagushi and M. Okamura, *Polyhedron*, 2011, **30**, 3284-3291.

[12] M. Wang, H. Fujiwara, T. Sugimoto, S. Noguchi and T. Ishida, *Inorg. Chem.*, 2005, **44**, 1184-1186.

[13] also with Metz as ligand: L. Wiehl, *Acta Cryst.*, 1993, **B49**, 289-303.

[14] F. A. Cotton and C. A. Murillo, *Inorg. Chem.*, 1975, **14**, 2467-2469.

[15] widely-used in cases where calorimetric data are available, see M. Sorai, *Chem. Rev.*, 2006, **106**, 976-1031.

[16] T. Nakamoto, Z. C. Tan and M. Sorai, *Inorg. Chem.*, 2001, **40**, 3805-3809; O. Roubeau, M. de Vos, A. F. Stassen, R. Burriel, J. G. Haasnoot and J. Reedijk, *J. Phys. Chem. Solids*, 2003, **64**, 1003-1013.

[17] M. Evangelisti, F. Luis, L. J. de Jongh and M. Affronte, *J. Mater. Chem.*, 2006, **16**, 2534-2549.
[18] L. J. de Jongh and A. R. Miedema, *Adv. Phys.*, 2001, **50**, 947-1170.
[19] T. Oguchi, *Phys. Rev.*, 1964, **133**, A1098-A1099.